ACTA MECHANICA SINICA, Vol.20, No.1, February 2004
The Chinese Society of Theoretical and Applied Mechanics
Chinese Journal of Mechanics Press, Beijing, China
Allerton Press, INC., New York, U.S.A.

ISSN 0567-7718

COUPLING OF ASSUMED STRESS FINITE ELEMENT AND BOUNDARY ELEMENT METHODS WITH STRESS-TRACTION EQUILIBRIUM

GUZELBEY Ibrahim H.† KANBER Bahattin AKPOLAT Abdullah

(*University of Gaziantep, Mechanical Engineering Department, Gaziantep* 27310, *Turkey*)

ABSTRACT: In this study, the stress based finite element method is coupled with the boundary element method in two different ways. In the first one, the ordinary distribution matrix is used for coupling. In the second one, the stress traction equilibrium is used at the interface line of both regions as a new coupling process. This new coupling procedure is presented without a distribution matrix. Several case studies are solved for the validation of the developed coupling procedure. The results of case studies are compared with the distribution matrix coupling, displacement based finite element method, assumed stress finite element method, boundary element method, ANSYS and analytical results whenever possible. It is shown that the coupling of the stress traction equilibrium with assumed stress finite elements gives as accurate results as those by the distribution matrix coupling.

KEY WORDS: coupling, assumed stress FEM, BEM, stress-traction equilibrium

1 INTRODUCTION

The main purpose of coupling of the finite element method (FEM) and boundary element method (BEM) is to take the advantages of both methods for the solution of various engineering problems. Both methods have some advantages in certain applications. While the BEM gives better results for the surface type problems like contact problems, FEM is more effective for the domain type problems.

In this study, the assumed stress finite element (SFE) method and the boundary element (BE) method are coupled using both distribution matrix (DMC) and stress-traction equilibrium equations (STC). The results of both methods are compared to each other and other methods and it is observed that the coupling by the stress-traction equilibrium gives more accurate stresses.

In the literature, it is seen that Zienkiewicz et al.[1] are one of the forerunners in studying the coupling process. They discussed the coupling in a general context. Later, Kelly et al.[2] proposed a method obtaining the symmetric stiffness matrices of the BE region which satisfy the equilibrium equation and applied the method to a number of field problems in fluid mechanics. Furthermore Felippa[3] used the coupling methods for a three dimensional structure submerged in an acoustic fluid. Beer[4] developed a general coupled BE and FE program in 1983. A number of special elements were included for the analysis of shell structures and joint/interfaces. The same author analysed the unbounded problems in elastostatics by the coupling method[5]. He claimed that the BEM is very efficient for unbounded problems in elastostatics.

The assumed stress finite elements were first proposed by Pian[6]. He derived the element stiffness matrices from an assumed stress distribution. Then Pin Tong[7] developed a new displacement hybrid finite element model for solid continua. Pian et al.[8] used a rational approach for assumed stress finite elements based on the Hellingner-Reissner principle. The same author studied the relations between incompatible displacement models and hybrid stress models[9]. He also proposed a rational approach for choosing stress terms for hybrid finite element formulations[10].

2 COUPLING PROCESS BY SUBREGIONAL TECHNIQUE

Although the subregion is a technique in

Received 21 November 2002, revised 10 July 2003
† E-mail: guzelbey@gantep.edu.tr

BEMs[11], the coupling process may also be thought as a subregional technique with the problem domain being divided into the two subdomains as BE and FE[12]. The stress-traction equilibrium approach may also be considered as a subregion technique due to the BE and FE subregions and the compatibility conditions on the interface line of two regions which is similar to the compatibility conditions in the subregion technique.

When the subregional coupling technique is used, the imaginary constraints, which are explained in Fig.1, must be considered at the interface line of the finite element and boundary element region. There are three types of boundary conditions. The first one includes the normal and tangential constraints at the interface line. The second one contains the normal constraints at the interface line. The last one includes only the tangential constraints at the interface. The type of the problem determines the type of imaginary boundary constraints. Some case studies are selected considering these different boundary constraints.

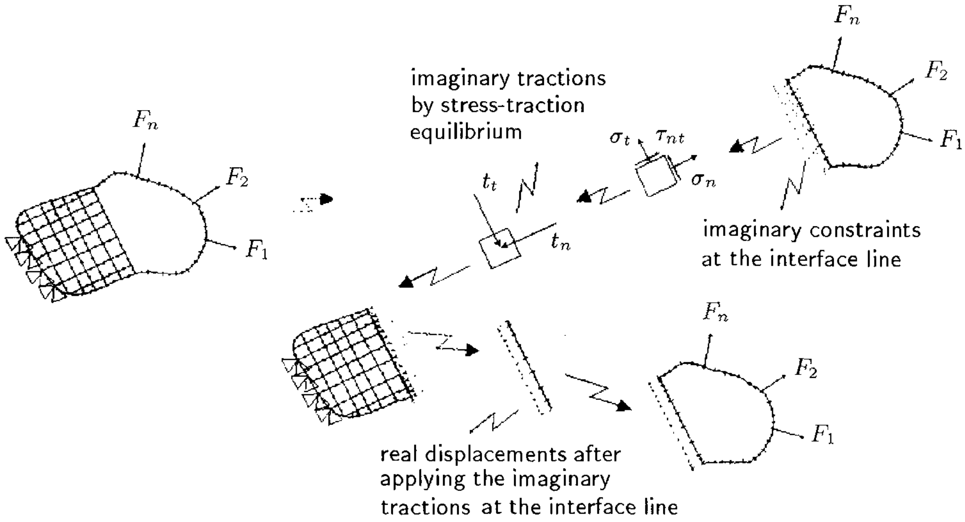

Fig.1 Imaginary constraints of coupling process for stress-traction equilibrium

2.1 Coupling by Distribution Matrix

The stress vector on an element is written by Pian[6] as follows

$$S = R\beta \tag{1}$$

where β is the stress coefficients, R the element surface coordinates.

The force and displacement relationship equation is also written by Pian[6] as follows

$$Q = kq \tag{2}$$

where

$$k = T^t H^{-1} T$$

$$T = \int_{A_2} R^t L \mathrm{d}A$$

$$H = \int_V P^t N P \mathrm{d}v$$

Equation (1) can be written in a new form by dividing the stress FEM region into two subregions as follows

$$\begin{vmatrix} Q_{\text{SFE}} \\ Q^*_{\text{SFE}_i} \end{vmatrix} = \begin{vmatrix} k_{\text{SFE}} & k_{\text{SFE}_i} \end{vmatrix} \begin{vmatrix} q_{\text{SFE}} \\ q^*_{\text{SFE}_i} \end{vmatrix} \tag{3}$$

where Q_{SFE} is the force vector at the SFE domain, $Q^*_{\text{SFE}_i}$ the imaginary internal reaction force vector at the interface line, q_{SFE} the displacement vector at the SFE domain, $q^*_{\text{SFE}_i}$ the imaginary displacement vector at the interface line.

The above equation may be solved for imaginary reaction force vector, $Q^*_{\text{SFE}_i}$.

After finding the imaginary reaction force vector at the interface line, the distribution matrix, M, may be used to transform it into the imaginary traction vector. So the distribution matrix[1] can be used as follows

$$Q^*_{\text{SFE}_i} = M q^*_{\text{SFE}_i} \tag{4}$$

Equation (3) can be rewritten in a new form similar to the general BE equation using Eq.(4)

$$\begin{vmatrix} I & M_{\text{SFE}_i} \end{vmatrix} \begin{vmatrix} Q_{\text{SFE}} \\ t^*_{\text{SFE}_i} \end{vmatrix} = \begin{vmatrix} k_{\text{SFE}} & k_{\text{SFE}_i} \end{vmatrix} \begin{vmatrix} q_{\text{SFE}} \\ q^*_{\text{SFE}_i} \end{vmatrix} \tag{5}$$

where $\boldsymbol{I}$ is the unit matrix, $\boldsymbol{M}_{\mathrm{SFE}_i}$ the distribution matrix at the interface line, $\boldsymbol{Q}_{\mathrm{SFE}}$ the force vector at the SFE domain, $\boldsymbol{t}^*_{\mathrm{SFE}}$ the imaginary traction vector at the interface line.

The general BE equation is as follows

$$\boldsymbol{Hq} = \boldsymbol{Gt} \tag{6}$$

It can also be rewritten to include the BE domain sub-matrix and interface BE sub-matrix as follows

$$\left|\boldsymbol{H}_{\mathrm{BE}_i} \quad \boldsymbol{H}_{\mathrm{BE}}\right| \left|\begin{matrix} \boldsymbol{q}_{\mathrm{BE}_i} \\ \boldsymbol{q}_{\mathrm{BE}} \end{matrix}\right| = \left|\boldsymbol{G}_{\mathrm{BE}_i} \quad \boldsymbol{G}_{\mathrm{BE}}\right| \left|\begin{matrix} \boldsymbol{t}^*_{\mathrm{BE}_i} \\ \boldsymbol{t}_{\mathrm{BE}} \end{matrix}\right| \tag{7}$$

where $\boldsymbol{t}^*_{\mathrm{BE}_i}$ is the imaginary traction vector, $\boldsymbol{q}_{\mathrm{BE}_i}$ the real displacement vector.

The traction compatibility must be satisfied for coupling purposes at the interface line as follows

$$\boldsymbol{t}^*_{\mathrm{SFE}_i} = -\boldsymbol{t}^*_{\mathrm{BE}_i} \tag{8}$$

Then Eq.(6) may be solved for the real displacement vector, $\boldsymbol{q}_{\mathrm{BE}_i}$. After finding the real displacement vector at the interface line, the displacement continuity requirement should be considered for coupling purposes

$$\boldsymbol{q}_{\mathrm{SFE}_i} = \boldsymbol{q}_{\mathrm{BE}_i} = \boldsymbol{q}_i \tag{9}$$

As a result, the general coupling equation can be written using Eqs.(5) and (7)

$$\left|\begin{matrix} \boldsymbol{k}_{\mathrm{SFE}} & \boldsymbol{k}_{\mathrm{SFE}_i} & \boldsymbol{0} \\ \boldsymbol{0} & \boldsymbol{H}_{\mathrm{BE}_i} & \boldsymbol{H}_{\mathrm{BE}} \end{matrix}\right| \left|\begin{matrix} \boldsymbol{q}_{\mathrm{SFE}} \\ \boldsymbol{q}_i \\ \boldsymbol{q}_{\mathrm{BE}} \end{matrix}\right| = \left|\begin{matrix} \boldsymbol{I} & \boldsymbol{M}_{\mathrm{SFE}_i} & \boldsymbol{0} \\ \boldsymbol{0} & -\boldsymbol{G}_{\mathrm{BE}_i} & \boldsymbol{G}_{\mathrm{BE}} \end{matrix}\right| \left|\begin{matrix} \boldsymbol{Q}_{\mathrm{SFE}} \\ \boldsymbol{t}_i \\ \boldsymbol{t}_{\mathrm{BE}} \end{matrix}\right| \tag{10}$$

2.2 Coupling by Stress-Traction Equilibrium

The coupling procedure is similar to the procedure mentioned in Sec.2.1. The distribution matrix, however, is not used for transformation.

The imaginary stress components can be found while writing Eq.(1) in terms of interface and domain sub-matrices and considering the imaginary constraints at the interface line as shown in Fig.1.

$$\left|\begin{matrix} \boldsymbol{S}^*_{\mathrm{SFE}_i} \\ \boldsymbol{S}_{\mathrm{SFE}} \end{matrix}\right| = \left|(\boldsymbol{R})_{\mathrm{SFE}_i} \quad (\boldsymbol{R})_{\mathrm{SFE}}\right| \left|\begin{matrix} \boldsymbol{\beta}^*_{\mathrm{SFE}_i} \\ \boldsymbol{\beta}_{\mathrm{SFE}} \end{matrix}\right| \tag{11}$$

Then these stress components can be transformed into tractions using stress-tractions equilibrium equations as follows

$$\begin{aligned} t^*_{xi} &= \left(\boldsymbol{S}^*_{xi} l + \boldsymbol{S}^*_{xyi} m\right) * th \\ t^*_{yi} &= \left(\boldsymbol{S}^*_{yi} m + \boldsymbol{S}^*_{yxi} l\right) * th \end{aligned} \tag{12}$$

where l, m are directional cosines of the interface, th is the thickness of the member.

After finding the imaginary tractions at the interface line, the general BE equation can be used to find the real interface displacements by following the way shown in Fig.1.

$$\left|\boldsymbol{H}_{\mathrm{BE}_i} \quad \boldsymbol{H}_{\mathrm{BE}}\right| \left|\begin{matrix} \boldsymbol{q}_{\mathrm{BE}_i} \\ \boldsymbol{q}_{\mathrm{BE}} \end{matrix}\right| = \left|\boldsymbol{G}_{\mathrm{BE}_i} \quad \boldsymbol{G}_{\mathrm{BE}}\right| \left|\begin{matrix} \boldsymbol{t}^*_{\mathrm{BE}_i} \\ \boldsymbol{t}_{\mathrm{BE}} \end{matrix}\right| \tag{13}$$

3 CASE STUDIES

Three different cases are used for the validations of the developed approaches. SFEM refers to the assumed stress finite element, DMC refers to coupling with distribution matrix and STC refers to coupling with stress-traction equilibrium.

3.1 Axially Loaded Bar

This is a simple plane stress problem. A thin axially loaded aluminum bar is considered ($E = 70\,\mathrm{GPa}$; $\nu = 0.3$). The dimensions are shown in Fig.2(a). The SFEM, BEM and coupling models can be seen in Figs.2(b), 2(c)and 2(d). Axial displacement and axial stress distributions against the length of the bar are

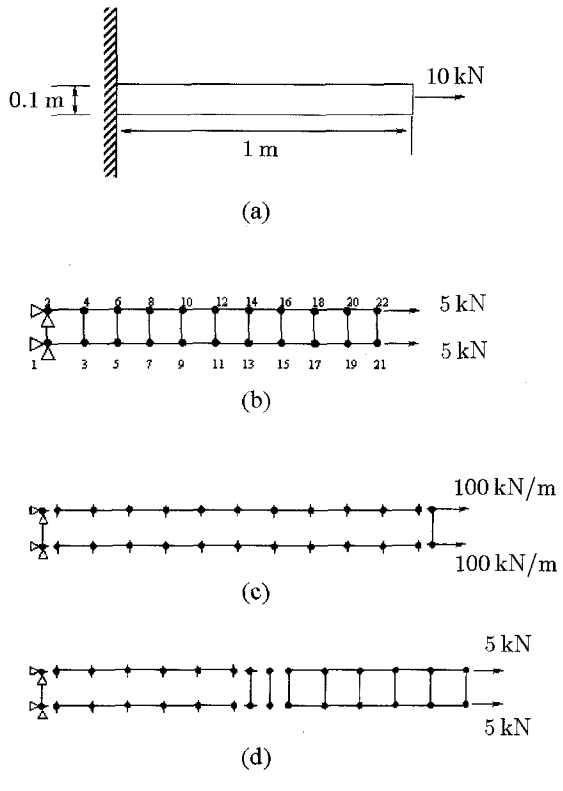

Fig.2 (a) Axially loaded bar, (b) Stress FEM model, (c) BEM model, (d) Coupling model shown in Figs.3 and 4. The results are exactly the same in all methods.

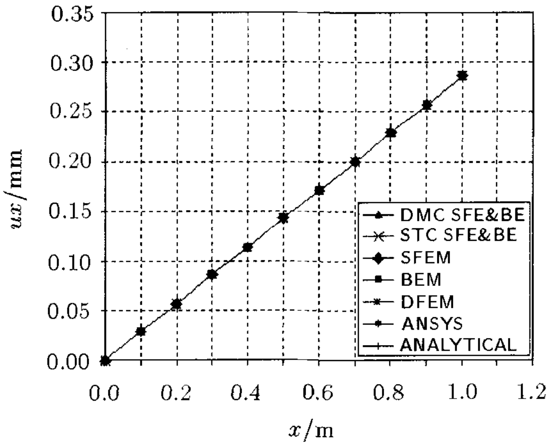

Fig.3 Axial displacement distribution along upper surface of bar

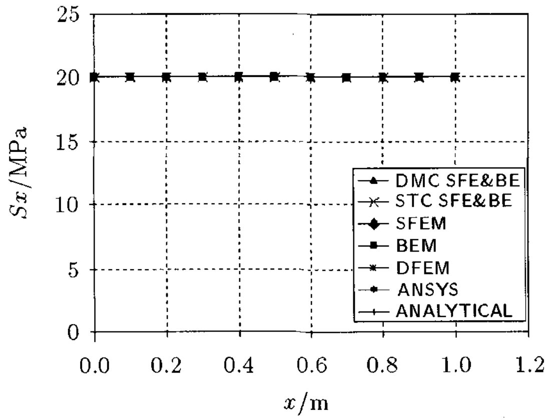

Fig.4 Axial stress distribution along upper surface of bar

3.2 Cantilever Beam

This case represents a cantilever beam under a vertical end load (Fig.5(a)). SFEM, BEM and coupling models are shown in Figs.5(b), 5(c) and 5(d). The beam is made of a steel alloy (E = 210 GPa; $\nu = 0.3$). The vertical displacements and axial stress distributions along the upper surface of the beam can be seen in Figs.6 and 7. The STC gives more accurate vertical displacement and axial stress results against the DMC and displacement based FEM.

3.3 Slideway Base

The slideway base under the action of weight of the inner part is considered. The material of the base is the gray cast iron with E = 100 GPa and $\nu = 0.211$. The whole assembly model is shown in Fig.8. Because of the symmetry, a half base part is modelled as shown in Fig.9. The SFEM, BEM and coupling model are

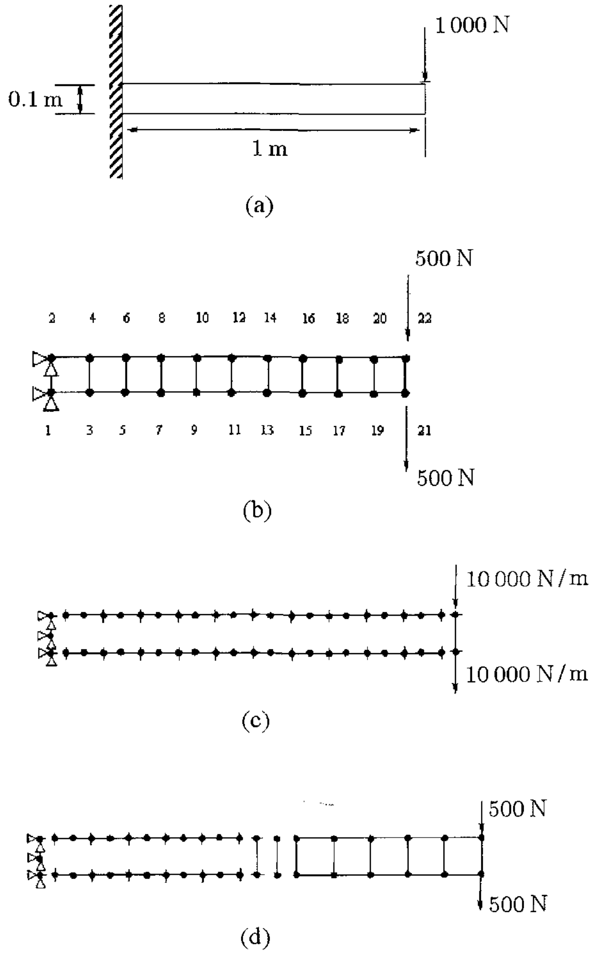

Fig.5 (a) Cantilever beam, (b) FEM model, (c) BEM model, (d) Coupling model

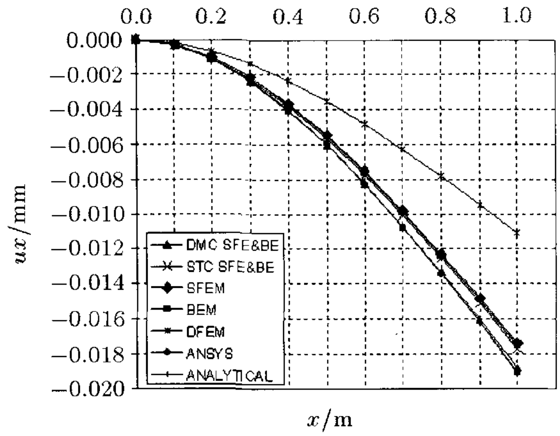

Fig.6 Vertical displacement distribution along upper surface of beam

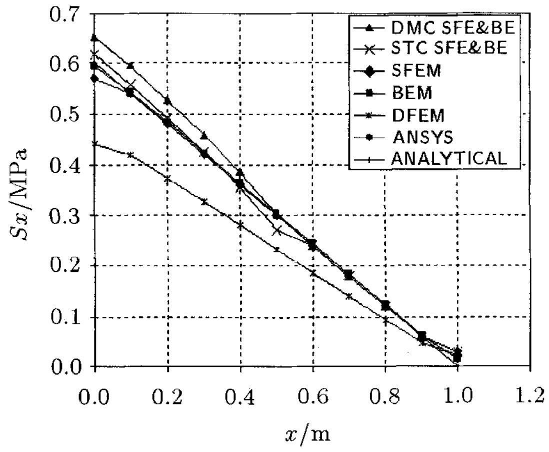

Fig.7 Axial stress distribution along upper surface of beam

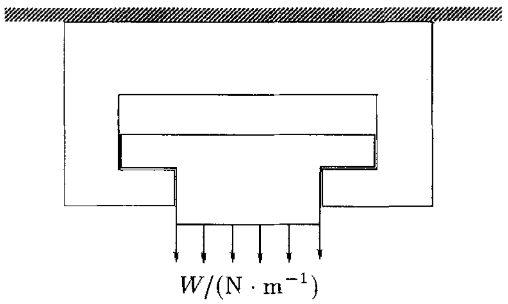

Fig.8 Slideway under the action of inner part weight

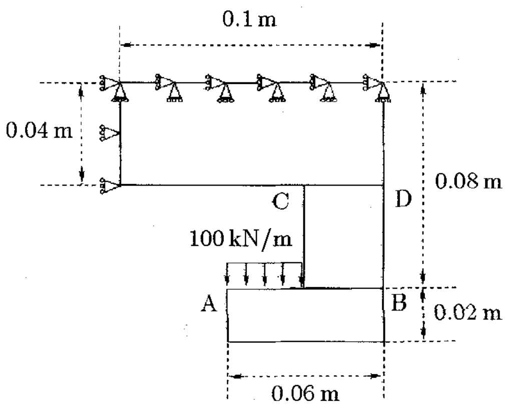

Fig.9 Half model of the slideway with boundary constraints

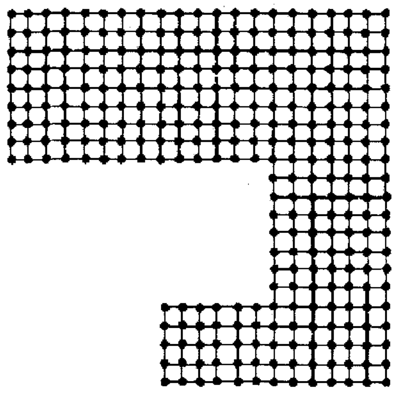

Fig.10 Stress FEM model of the slideway base

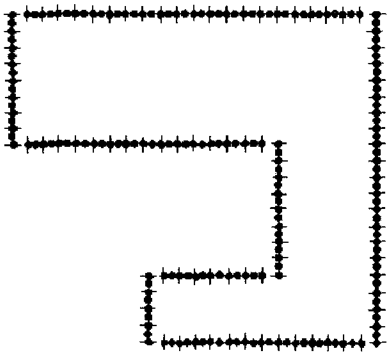

Fig.11 BEM model of the slideway base

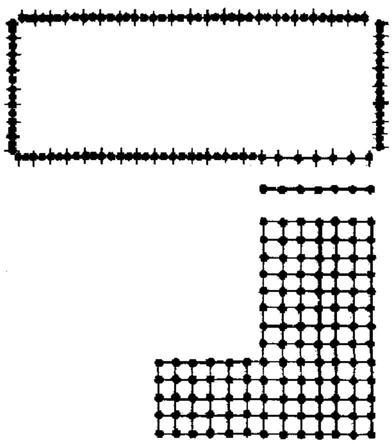

Fig.12 Coupling model of the slideway base

shown in Figs.10, 11 and 12. The vertical displacement and axial stress distributions on the line AB and vertical stress distribution on the line CD are shown in Figs.13, 14 and 15. The BEM stresses on lines AB and CD are not accurate. This, of course, comes from the characteristics of the model. The errors may be reduced using the integration cells. In this study, however, the errors are reduced in the coupling results. The STC coupling results are in good agreement with SFEM, Displacement FEM and ANSYS against DMC results.

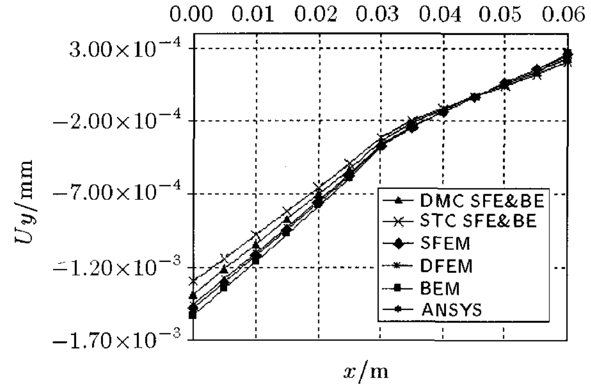

Fig.13 The vertical displacement (Uy) distribution along line AB on the slideway base

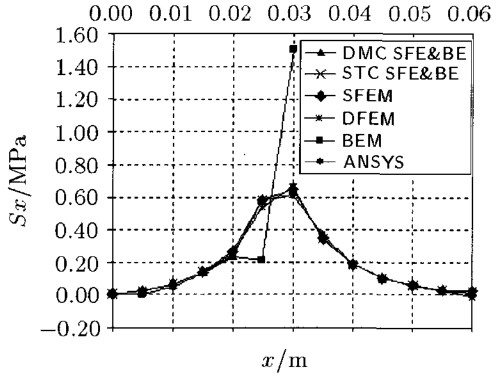

Fig.14 The axial stress (Sx) distribution along line AB on the slideway base

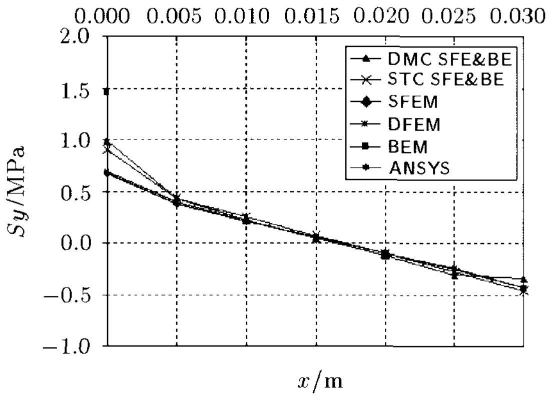

Fig.15 The vertical stress (Sy) distribution along line CD on the slideway base

4 CONCLUSION

This study shows that the STC gives more accurate stress results than the DMC even in complicated cases. The reason of this, of course, comes from using the stresses, obtained by assumed stress finite elements, to find the nodal tractions at the interface line. So STC approach may be used safely for more complicated cases. In fact, some more engineering cases may be considered to show the reliability of the STC.

Acknowledgement Authors wish to thank TUBİTAK-BAYG for scholarship of B. Kanber during this study.

REFERENCES

1 Zienkiewicz OC, Kelly DW, Bettess P. The coupling of the finite element method and boundary solution procedures. *Int J Numer Meth Engng*, 1977, 11: 355~375

2 Kelly DW, Mustoe GGW, Zienkiewicz OC. Coupling Boundary Element Methods with Other Numerical Methods, Developments in Boundary Element Methods. Vol-1, Chap 10, London: Applied Science Publishers, 1979

3 Felippa CA. Interfacing finite element and boundary element discretization. *Appl Math Modelling*, 1981, 5: 383~386

4 Beer G, Meek JL. The coupling of the boundary and finite element methods for infinite domain problems in elastoplasticity. In: Brebbia CA ed. Proc 3rd Inter Sem Boundary Element Methods, Irvine, Berlin: Springer, 1981. 575~591

5 Beer G. Finite element, boundary element and coupled analysis of unbounded problems in elastostatics. *Int J Numer Meth Engng*, 1983, 19: 567~580

6 Pian THH. Derivation of element stiffness matrices by assumed stress distributions. *AIAA*, 1964, 2: 1333~1376

7 Tong P. New displacement hybrid finite element models for solid continua. *Int J Numer Meth Engng*, 1970, 2: 73~83

8 Pian THH, Sumihara K. Rational approach for assumed stress elements. *Int J Numer Meth Engng*, 1984, 20: 1685~1695

9 Pian THH, Tong P. Relations between incompatible displacement model and hybrid stress model. *Int J Numer Meth Engng*, 1986, 22: 173~181

10 Pian THH, Wu CC. A rational approach for choosing stress terms for hybrid finite element formulations. *Int J Numer Meth Engng*, 1988, 26: 2331~2343

11 Guzelbey IH. Finite and boundary element analysis of elasto-plastic finite strain contact problems. [Ph D Dissertation]. Cranfield Institute of Technology, UK, 1992

12 Kanber B. A new procedure for finite and boundary element methods. [Ph D Dissertation]. University of Gaziantep, Turkey, 2001